

APOSR-TR- 71-0853

# FIFTH INTERNATIONAL CONFERENCE ON MAGNETOHYDRODYNAMIC ELECTRICAL POWER GENERATION

AD 721 455

**FACTORS EFFECTING THE PERFORMANCE OF DIAGONAL  
CONDUCTING WALL OPEN CYCLE MHD GENERATORS**

**Y. C. L. Wu, L. Crawford, R. Shanklin,  
J. Muehlhauser, D. Molnar  
and J. B. Dicks**

**The University of Tennessee Space Institute  
Tullahoma, Tennessee 37388**

*F44620-69-C-0031*

**This document has been approved for public  
release and sale; its distribution is unlimited.**

Organised jointly by

**THE OECD EUROPEAN NUCLEAR ENERGY AGENCY**

and

**THE INTERNATIONAL ATOMIC ENERGY AGENCY**

Reproduced by  
**NATIONAL TECHNICAL  
INFORMATION SERVICE**  
Springfield, Va. 22151

**MUNICH**  
19th-23rd April 1971

**D D C**  
**RECORDED**  
APR 14 1971  
**RECORDED**

D

19

**FACTORS EFFECTING THE PERFORMANCE OF DIAGONAL  
CONDUCTING WALL OPEN CYCLE MHD GENERATORS\***

**Y. C. L. Wu, L. Crawford, R. Shanklin,  
J. Muehlhauser, D. Molnar  
and J. B. Dicks**

**The University of Tennessee Space Institute  
Tullahoma, Tennessee**

**ABSTRACT**

A systematic study has been undertaken to attempt to evaluate gross factors effecting the overall performance of series connected generators. These factors include combustor performance, chemistry, magnetic field strength, Mach number, and electrode segmentation. Because of the importance involved in scaling small MHD generators up to the sizes required for large central power plants and other applications, an attempt was made to investigate the scaling parameters by varying the magnetic field in a wide range and by changing the seed percentage and Mach number of flow. The results indicated the scaling law for the magnetic field is of the form  $(B-V_d/ud)^2$ . Dimensional scaling was investigated by varying the segmentation ratio of electrode length to channel height. The results show that when the electrode length divided by the channel height is changed from the neighborhood of .12 to the neighborhood of .25 then the generator power output decreases by 15 percent over the entire load spectrum. Other studies involving gross generator behavior include an investigation of the effect resulting from the deposit of aluminum oxide and other combustion materials on the walls of the generator. No deterioration of performance was noted during this process. The addition of the powdered aluminum improved the generator performance. Powdered coal was burned and produced satisfactory power output. During the course of the experimental study, it was found that both the injector head and combustor are very critical to the performance of the generators.

---

\*Sponsored in part by the Air Force Office of Scientific Research, Office of Aerospace Research, USAF, under Contract F44620-69-C-0031.

## INTRODUCTION

In this paper we shall present an experimental study which attempts to evaluate gross factors effecting the overall performance of series connected generators. The various parameters that are included in this study are the magnetic field strength, types of fuel, seed and solid additives (aluminum and coal), electrode segmentation, different injector heads, Mach numbers, as well as types of generators.

The generators used in this experimental study were made of electrolytic copper of heat sink design. There are approximately sixty pairs of electrodes (depending on type of generators) insulated from each other by ceramic fiber paper of .05 cm thickness. The electrode length is approximately 1.53 cm. The overall dimensions of the generators are approximately 9.5 cm x 20.5 cm x 120 cm. The walls perpendicular to the magnetic field remain parallel while the other walls each diverge at an angle of  $1.2^\circ$ . The plasma was produced by burning hydrocarbon fuel (kerosene was used for most of the experiments) and seed with gaseous oxygen in a rocket type combustion chamber. Detailed description of the experimental setup may be found in references 1 and 2.

## GENERATOR PERFORMANCE AND SCALING OF MAGNETIC FIELD STRENGTH

The series connected generator was first studied by de Montardy<sup>[3]</sup> and later by Dicks, et al<sup>[4]</sup> and Wu, et al<sup>[5]</sup>. It is desirable to tabulate the various interesting quantities, such as current density, etc. as functions of the generator conditions (velocity, cross-sectional area, magnetic induction, load, etc.). The following table lists all the interesting quantities involving generator performance. In this table the magnetic field is applied in the negative z-direction and gas velocity in the positive x-direction. R is load resistance,  $\Delta = V_d/uBd$  is the dimensionless voltage drop,  $\Omega$  is Hall parameter,  $\phi = \tan \theta$  where  $\theta$  is the angle between the side wall and the y-axis, the other notations are conventional.

The maximum power density condition is found from the table to be

$$I_{MP} = \frac{\sigma AuB(1 - \Delta)(\Omega + \phi)}{2(1 + \Omega^2)} \quad (1)$$

$$E_{x_{MP}} = - \frac{uB(1 - \Delta)(\Omega + \phi)}{2(1 + \phi^2)} \quad (2)$$

TABLE I. SUMMARY OF MHD EQUATIONS FOR DCW GENERATORS

	In terms of Resistance R	In terms of Total Current I
$J_x$	$\sigma u B(1-\Delta) \frac{\Omega L - \phi \sigma A R}{(1+\Omega^2)L + \sigma A R(1+\phi^2)}$	$\frac{(1+\Omega\phi)I - A\sigma u B(1-\Delta)\phi}{A(1+\phi^2)}$
$J_y$	$\sigma u B(1-\Delta) \frac{L + \sigma A R}{(1+\Omega^2)L + \sigma A R(1+\phi^2)}$	$\frac{(\phi - \Omega)I + A\sigma u B(1-\Delta)}{A(1+\phi^2)}$
$E_x$	$-u B(1-\Delta) \frac{\sigma A R(\Omega + \phi)}{(1+\Omega^2)L + \sigma A R(1+\phi^2)}$	$\frac{(1+\Omega^2)I - A\sigma u B(1-\Delta)(\Omega + \phi)}{\sigma A(1+\phi^2)}$
$E_y$	$\phi E_x$	$\phi E_x$
$I = A(j_x + \phi j_y)$	$\sigma u B(1-\Delta) \frac{A L(\Omega + \phi)}{(1+\Omega^2)L + \sigma A R(1+\phi^2)}$	$I$
$\vec{P} = \vec{J} \cdot \vec{E}$	$-\frac{\sigma A R}{L} \left[ \frac{u \Omega(1-\Delta)(\Omega + \phi)L}{(1+\Omega^2)L + \sigma A R(1+\phi^2)} \right]^2$	$-\frac{I}{\sigma A^2(1+\phi^2)} \left[ A\sigma u B(1-\Delta)(\Omega + \phi) - \phi(1+\Omega^2)I \right]$
$\eta = \frac{\vec{J} \cdot \vec{E}}{\vec{U} \cdot (\vec{J} \times \vec{B})}$	$(1-\Delta) \frac{\sigma A R L(\Omega + \phi)^2}{(L + \sigma A R) \left[ (1+\Omega^2)L + \sigma A R(1+\phi^2) \right]}$	$\frac{I}{A\sigma u B} \left[ \frac{A\sigma u B(1-\Delta)(\Omega + \phi) - (1+\Omega^2)I}{A\sigma u B(1-\Delta) + (\phi - \Omega)I} \right]$

W

The corresponding power density is

$$P_{MP} = \frac{\sigma [uB(1 - \Delta)(\Omega + \phi)]^2}{4(1 + \phi^2)(1 + \Omega^2)} \quad (3)$$

and the load that is required to reach the maximum power density condition is

$$R_{MP} = \frac{L(1 + \Omega^2)}{\sigma A(1 + \phi^2)} \quad (4)$$

Figure 1 shows the dimensionless maximum power density for various types of generators at different Hall parameters. It is clear that at low Hall parameters, the Hall generator does not operate satisfactory at all. From this figure, one can choose the desired Hall parameter for a given generator, or for a specified Hall parameter (as restricted by pressure and magnetic field strength) a designer may choose the type of generator to build. In the case of wide variation of Hall parameters, it seems that the 60° channel ( $\phi = .577$ ) is the best choice since it is less sensitive to the Hall parameter at maximum power density condition. Figure 2 shows the experimental voltage-current characteristics for both the Hall and 60° channel at  $B=2.22$  Tesla. It is clear that the Hall generator does not perform well as compared to the 60° channel under the same conditions.

From the above table, we see that the power density is proportional to  $\sigma[uB(1 - \Delta)]^2$  for a given load. The dimensionless voltage loss  $\Delta$  is defined as  $V_d/uBd$  where  $V_d$  is the voltage drop,  $u$  is velocity,  $B$  is magnetic induction and  $d$  is distance between electrodes. For a given generator operating at limited ranges of magnetic induction, one expects that the voltage drop  $V_d$  is nearly constant and the plasma properties remain nearly unchanged. Therefore, for a given load  $R$ , we have

$$\frac{P_1}{P_2} = \frac{B_1^2(1 - \Delta_1)^2}{B_2^2(1 - \Delta_2)^2} = \frac{(B_1 - \frac{V_d}{ud})^2}{(B_2 - \frac{V_d}{ud})^2} \quad (5)$$

It is previously determined that at  $B = 2$  Tesla,  $\Delta = V_d/uBd = .56$ <sup>[5]</sup>, thus, we can find

$$\frac{P_1}{P_2} = \frac{1}{.1936} \left( \frac{B_1}{B_2} - .56 \right)^2 = 1.29(B_1 - 1.12)^2 \quad (6)$$

where  $B_2 = 2$  Tesla,  $P_2$  is the power density at  $B_2$  and  $P_1$  is the power density at  $B_1$ . Figure 3 shows  $P_1/P_2$  as plotted based on the above relation<sup>1</sup>. The experimental points for both the Hall and 60° channel at  $10\Omega$  load give strong support of the above scaling law.

## INVESTIGATION OF SOLID FUEL ADDITIVES

**Powder Injection System Design and Operation.** In order to obtain the capability of injecting various powdered compounds directly into the combustion chamber for the subsequent study of the effects of such compounds upon the operation of an MHD generator, a powder feed system was designed and fabricated. The principle upon which the design was based is called dense-phase flow which is a particulate medium being conveyed by the viscous drag of a carrier gas. The principal characteristic of dense-phase flow is a high weight ratio of particulate flow to gas flow. Certainly dense-phase flow, in contrast to dilute-phase flow, has a weight ratio of 5:1 (48 kilograms of particulate matter per cubic meter of hydrogen carrier gas) although higher values are more desirable for our purposes. A schematic diagram of the injection system is shown in Figure 4.

The carrier gas selected for use is gaseous hydrogen which has several advantages over other possible choices. First, it is inert with the powder compounds used (aluminum, coal, char, and potassium nitrate); second, because it has a high fuel value, it does not act as a flame depressant as would another choice such as nitrogen or methane-air combustion products (used in boiler coal firing); third, because dense-phase flow is partly volume dependent, it is felt that higher weight ratios can be obtained than with another fuel such as methane.

The hopper is placed so that the flow is counter-gravity. Preliminary tests showed that the entrance to the exit line tended to clog when the flow was directed vertically downward. To reduce the line losses the hopper is located as close to the combustion chamber as is practicable. The close coupling of combustor and hopper also precludes the necessity of accurate timing of hopper actuation in the firing sequence. With regard to introducing the carrier gas into the hopper care must be exercised to insure that the mixing of powder and gas occur under highly turbulent conditions. During early tests the gas was introduced along the axis of the hopper, and even though a diffuser tube directing the flow radially outward was used a "tunneling" effect in the powder occurred with the result that toward the end of a test run there was almost no particulate flow. When the carrier gas was introduced horizontally across the hopper axis the particulate flow remained more nearly uniform during a test run.

Preliminary operating characteristics of the system were obtained under actual firing conditions. An attempt to calibrate the system under cold flow conditions was made by setting the pressure differential between hopper and atmosphere at the same value as would be encountered under actual operations. During subsequent firings it was found that dense-phase flow apparently depends on the level of pressure as well as the pressure gradient, thereby invalidating calibration data thus obtained.

The technique of system operation was as follows, and reference can be made to the system diagram in Figure 4. Prior to operation the hopper was pressurized with regulated hydrogen

and was, typically, at a pressure level approximately four to eight atmospheres greater than that pressure expected in the combustion chamber. The on-off pneumatic valve in the line into the combustion chamber was actuated at that time in the firing sequence at which the potassium seed valve was activated. The valve was shut off at the end of approximately five seconds of generator operation in order to more graphically see the difference between generator operation with and without powder injection. Typical values of particulate flow varied between 40 and 100 grams per second. This value is between 5 and 15 percent of the total flow rate of the generator working fluid. The maximum weight ratio of particulate to carrier gas flow was observed to be approximately 10:1.

Repeated calibrations in place produced results for aluminum and coal which were repeatable no closer than  $\pm 10$  percent. It was found that the particulate flow was dependent upon the powder volume relative to that of the hopper. Subsequently, the hopper volume was increased by a factor of approximately five with somewhat better results. Particle size and weight are also a factor to be considered. The powdered aluminum particles were approximately five microns in diameter while the coal particles were approximately seventy microns in diameter. Although coal has a lower density than aluminum it was felt that the greater surface area of the smaller aluminum particles would produce greater drag thereby resulting in higher aluminum flow rates. The reverse was observed, the coal flow being approximately 30 percent higher. When 300 micron diameter char was used in the hopper no flow at all was observed. Although of almost the same density as coal the surface area of the char was obviously insufficient to produce drag great enough to produce a sustained flow.

It is, of course, obvious that much development work needs to be done before the system reaches the desired level of reliability and repeatability. It is felt, however, that this development lies in the area of operating technique and that no serious conceptual barriers exist. The limits of the operating parameters of particle size, weight, carrier flow rate, and hopper pressure need to be firmly established. In addition other carrier gases need study as the merits of a particular carrier may vary from application to application, particularly with regard to weight ratio optimization. It is felt, however, that the feasibility of this technique of injecting powder into a combustor for use in an MHD generator has been demonstrated in ample fashion.

Injector Configuration. Two combustor injector head configurations were used in the series of powder injection experiments. The first configuration is shown in Figure 5. The powder is injected along the axis of the combustion chamber. The powder injector is integral with the hydrogen-air ignitor whose ports surround the powder injection line. The liquid fuel and seed solution are injected around the outer perimeter of the injector head in two concentric rings of six ports each. The oxygen ports are in a series of concentric rings located between the fuel and powder injector port.

The second injector head configuration is shown in Figure 6. The powder is injected through two ports diametrically opposed and located on the outer perimeter of the injector head. The injection is directed toward the combustor axis at an angle of  $45^\circ$ . The outer fuel, fuel-seed, and oxygen ports are identical to those of the first configuration. The hydrogen-air ignitor port is located on the combustor axis and is surrounded by a ring containing four fuel ports. This injector head is the standard configuration used in all previous experiments with only the modification for powder injection added.

Generator Operating Results with Powder Injection. Both injector head configurations were tested with The University of Tennessee Space Institute  $60^\circ$  diagonal conducting wall generator. The nominal magnetic field was 2.2 tesla. Four different particulate compounds were used: aluminum, coal, char, and potassium nitrate. Of these four, the char particles were too coarse and resulted in essentially no particulate flow. The potassium nitrate particles tended to clump together thereby producing a very erratic flow, and no meaningful results were obtained. Due to scheduling restrictions experiments with these two powder compounds were abandoned for the present.

Meaningful results were obtained using aluminum and coal. A total of 18 test runs were made with these compounds in which particulate matter was injected into the combustion chamber: four aluminum and one coal using axial injection, and four aluminum and nine coal using injection on the outer perimeter. Of these, 11 have been selected as suitable for comparison and are discussed herein.

The results from aluminum injections are shown in Figure 7. The aluminum flow rate was approximately 65 g/sec with a weight ratio of 6.8:1; the differential pressure between hopper and combustor was eight atmospheres. The data points at short circuit and five ohms result from using center injection. Data at 10 ohms were taken using perimetrical injection. The closed data points are those obtained during aluminum injections and the open points were taken after the particulate flow had been stopped. In all cases a significant drop in power can be seen to have occurred when the aluminum flow ceased, all other flow rates remaining constant. A graph of total current taken from an oscillograph trace for a typical test run is shown in Figure 8 and more graphically illustrates this observation.

An additional observation can be made about the relative efficiency of the two injector heads. The elimination of the center fuel ports from the axial injector was inimical to the operation of the generator. Extensions of the V-I curves from short circuit and five ohm conditions to the 10 ohm load line clearly show this. An additional data point with no powder injection at all is given for comparison with data from the perimetrical injection at the 10 ohm load and tends to reinforce the observation. Subsequent tests using coal (see Figure 7) also lend support to this.

The results from adding coal to the combustion chamber also are shown in Figure 7. With the exception of a single data

point at a 10 ohm load all data were obtained using perimetrical injection. The repeatability of the data at the 10 ohm line is particularly gratifying in view of the preliminary nature of the experiments. During these tests the coal flow rate was approximately 95 g/sec at a weight ratio to hydrogen of about 10:1. The hopper/combustor differential pressure was set at approximately eight atmospheres.

Three observations should be noted about the experiments with aluminum and coal. First, the work herein reported is preliminary in nature. Refinement of technique and optimum fuel oxygen mixtures were not the object of these studies; work should and is proceeding in these areas. The primary purpose of demonstrating feasibility was achieved and the basic operating guidelines established.

Second, the power levels reached are not as high as previously achieved with the same equipment. Because these series of experiments were posterior to an earlier series which utilized the same equipment, deterioration of the MHD generator channel with regard to electrical quality was expected and the lower power levels predictable.

Third, analysis has shown that the size of the combustion chamber was not large enough for the efficient combustion of the particulate matter. Of course, burner optimization is extremely important in order to achieve the good combustion so necessary for high power in an MHD generator.

#### EXPERIMENTAL STUDY USING KEROSENE AND POTASSIUM HYDROXIDE

Numerous tests were made with kerosene seeded with potassium hydroxide dissolved in alcohol. In these tests, the nominal flow rates are: Oxygen - .57 kg/sec; RP1 - .164 kg/sec; Alcohol-KOH - .063 kg/sec; Total mass flow rate - .8 kg/sec.

The combustion chamber pressure is  $45 \pm 1$  psia for the Mach 1.6 nozzle and  $65 \pm 1$  psia for the Mach 2 nozzle. Figure 2 shows the current-voltage characteristics of Hall and  $60^\circ$  DCW generators. For the  $60^\circ$  generator, two Mach numbers and two segmentation ratios are shown. Both of these generators have an average electrode length to channel height ratio of about .12, whereas the longer electrodes were achieved simply by shorting every adjacent electrode so that the effective electrode is twice as long. The coarse segmentation channel produces about 15% less power as compared to the original channel as expected from theory [5]. At the same mass flow rate the higher Mach number flow gives slightly higher power output than the Mach 1.6 case. This is because that at the same mass flow rate, the Mach 2 nozzle produces a flow with higher velocity but lower temperature and pressure, thus, the factor  $\sigma u^2$  is probably slightly changed. If the exit temperature and pressure of the Mach 2 nozzle are equal to those at the Mach 1.6 nozzle exit, significant increase in power output is expected.

In addition to the two supersonic nozzles, a subsonic nozzle of Mach .8 was also used in the experiment. Preliminary

study was made concerning flow rates, chamber pressure, etc. The plasma exhausts directly into atmosphere which required the combustion chamber pressure to be low in order to maintain subsonic flow in the channel. Two plates were added to the diffuser exit to choke the flow. This allowed us to use higher chamber pressure.

Figure 9 shows the dimensionless electrode drop  $\Delta$  as functions of the load current. The average plasma conditions used to compute  $\Delta$  are listed below:  $\langle B \rangle = 2.17$  Tesla,  $\langle \Omega \rangle = 1.27$ ,  $\langle \sigma \rangle = 17$  mhos/m,  $\langle u \rangle = 1500$  m/sec,  $\langle A \rangle = .645 \times 10^{-2} \text{m}^2$ ,  $\langle d \rangle = .127\text{m}$ ,  $L = .805\text{m}$ . This figure shows that the Hall generator has higher electrode drops, and for a given generator angle (say,  $60^\circ$  channel), the electrode drop increases with increasing segmentation ratio. The electrode drop decreases with increasing load current (corresponds to decreasing load resistance). For the Hall generator, the electrode drop is almost linearly proportional to the load current. However, for the  $60^\circ$  channel, the electrode drop seems to level at high load resistance (or low load current). The reason for the different behavior between the Hall and DCW generators are yet to be uncovered.

Figure 6 shows both the dimensionless and actual voltage drops of a typical run of the Hall generator. The DCW generator has a lower electrode drop than that of the Hall generator. However the increasing of the electrode drop along the channel length trend is alike for both types of generators. This trend is probably due to the colder channel wall downstream and the growth of the boundary layer. The large voltage drop associated with the cold electrode in a combustion plasma are also observed by Kessler and Eustis<sup>[6]</sup> among others.

#### STUDY OF DIFFERENT FUELS AND SEEDS

Exploratory investigations have been carried out using fuels and seeds other than our conventional kerosene with alcoholic KOH. The powdered fuels, aluminum and coal, and powdered seed,  $\text{KNO}_3$ , have been mentioned in a previous section. The other liquid fuel tested was benzene, and the liquid solutions of seed included  $\text{K}_2\text{CO}_3$  (50 percent in water) and  $\text{Cs}_2\text{CO}_3$  (65 percent in water). The  $\text{K}_2\text{CO}_3$  with kerosene gave comparable conductivities to alcoholic KOH, while the conductivity with  $\text{Cs}_2\text{CO}_3$  solution and kerosene was double that obtained with alcoholic KOH. Use of benzene with alcoholic KOH gave about 50 percent higher conductivities than kerosene fuel.

A limited number of power experiments were carried out using the Mach 2 nozzle with the  $60^\circ$  DCW channel using kerosene, benzene and various seeds. The best steady power obtained was with benzene and alcoholic KOH, at 64 kw, about 30 percent above comparable values with kerosene and alcoholic KOH. Results with benzene and cesium carbonate were very erratic, although brief periods of power at over 70 kw were observed. It appears that  $\text{Cs}_2\text{CO}_3$  precipitates from the concentrated solution, and possibly should be added as powder or in a more dilute solution.

## CONCLUSION

A systematic study was made to uncover some of the factors effecting the gross behavior of the generator. It is found that the scaling law for the magnetic field is of the form  $(B - V_d/ud)^2$ , where  $V_d$  is the average electrode drop. Over limited ranges of the magnetic field strength,  $V_d$  stayed fairly constant for a given load. The losses in the generator increase with increasing segmentation ratio. Powdered fuel additives were used and it was found that aluminum increases the power output whereas the powdered coal addition produced comparable power as pure kerosene used alone.

During the course of the powder injection tests it was discovered that the thorough mixing of the various fuel and seed streams is very important. The sensitivity of the generator performance is strikingly shown in the experimental data from the two injector heads and points out the importance of good combustor characteristics for generator operation.

## REFERENCES

1. Dicks, J. B., et al. "An Experimental and Theoretical Comparison of the Performance of Diagonal Wall Generators," Paper SM-74/169, Proceedings of the International Symposium on MHD Electrical Power Generation, Salzburg, Austria, 1966.
2. Martin, J. F., "Current Distribution in a Hall Generator Electrode," M. S. Thesis, The University of Tennessee, August, 1970.
3. de Montardy, A., "MHD Generator with Series-Connected Electrodes," Paper 19, Proceedings of International Symposium on MHD Electrical Power Generation, Newcastle Upon Tyne, England, 1962.
4. Dicks, J. B., et al. "Characteristics of a Family of Diagonal Conducting Wall MHD Generators," Proceedings of Eighth Symposium on Engineering Aspects of MHD, Stanford University, 1967.
5. Wu, Y. C. L., et al. "MHD Generator in Two-Terminal Operation," AIAA Journal, Vol. 6, No. 9, 1968.
6. Kessler, R., and Eustis, R. H., "Effects of Electrode and Boundary-Layer Temperature on MHD Generator Performance," AIAA Journal, Vol. 6, No. 9, 1968.

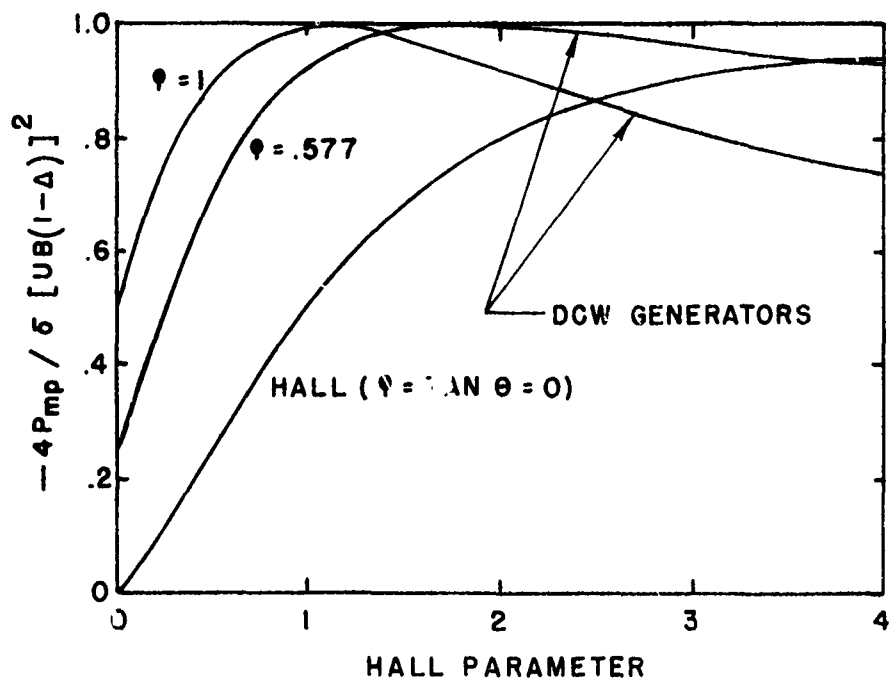
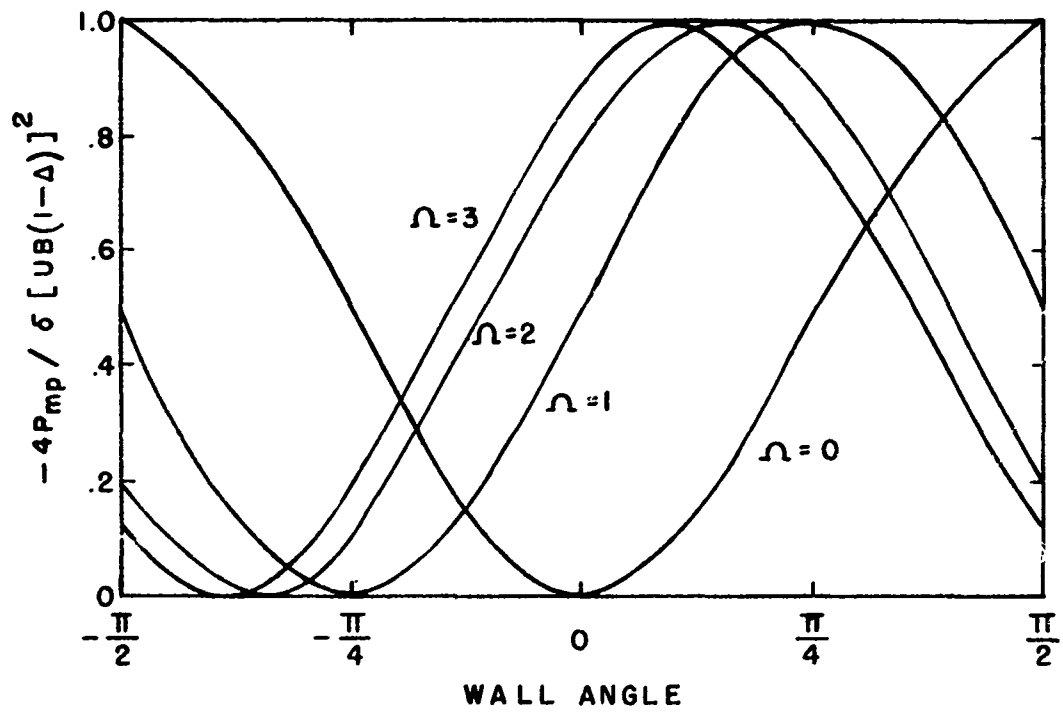


Figure 1. Dimensionless maximum power density at various Hall parameters and wall angles.

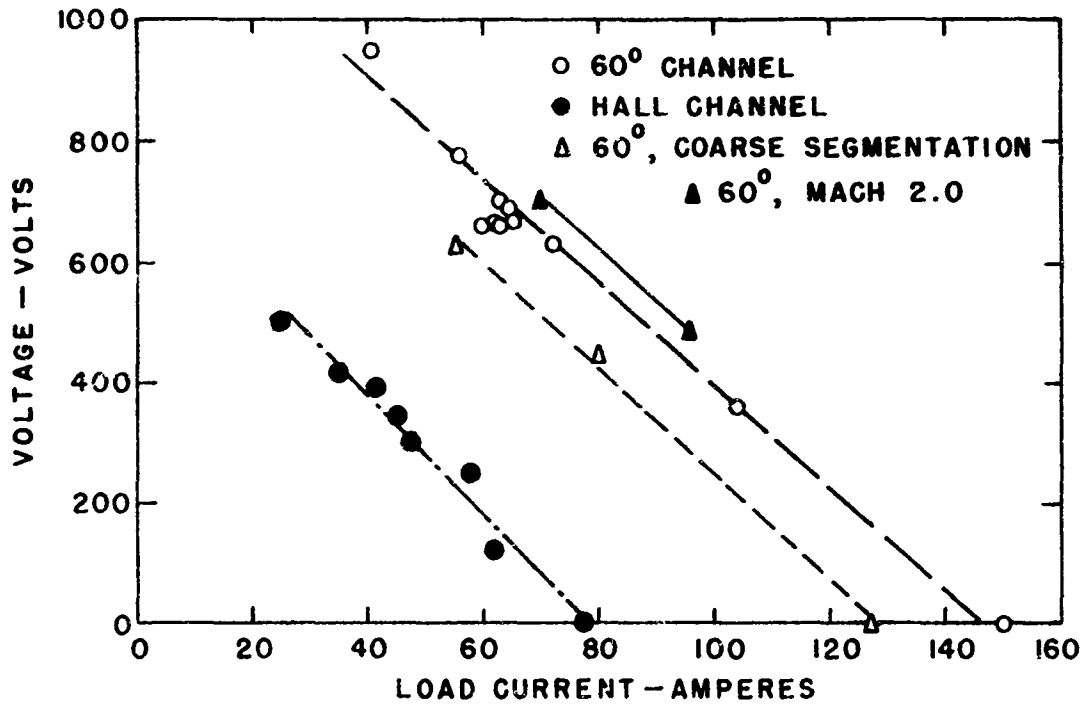


Figure 2. Experimental voltage-current characteristics for the 60° and Hall generators using kerosene fuel and KOH seeding at a flow rate of 0.8 kg/sec with a magnetic field of 2.2 tesla.

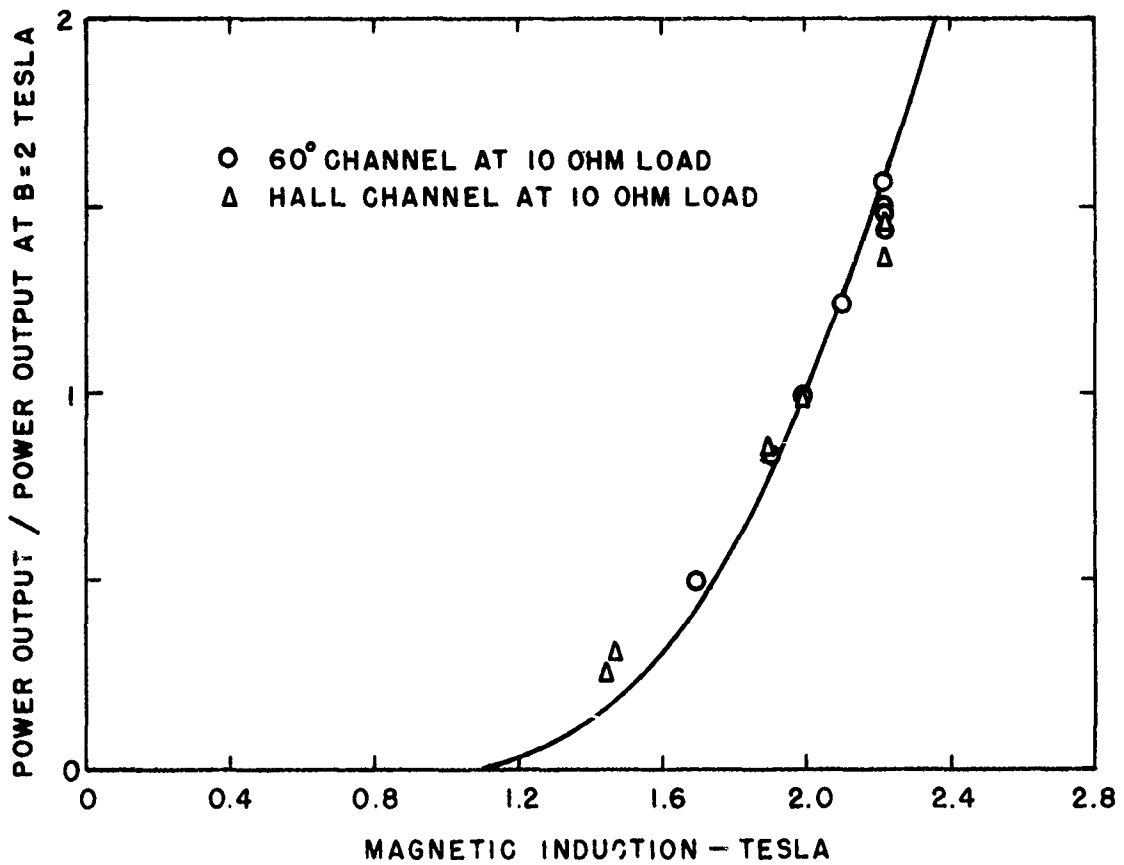


Figure 3. Power output as a function of magnetic induction.

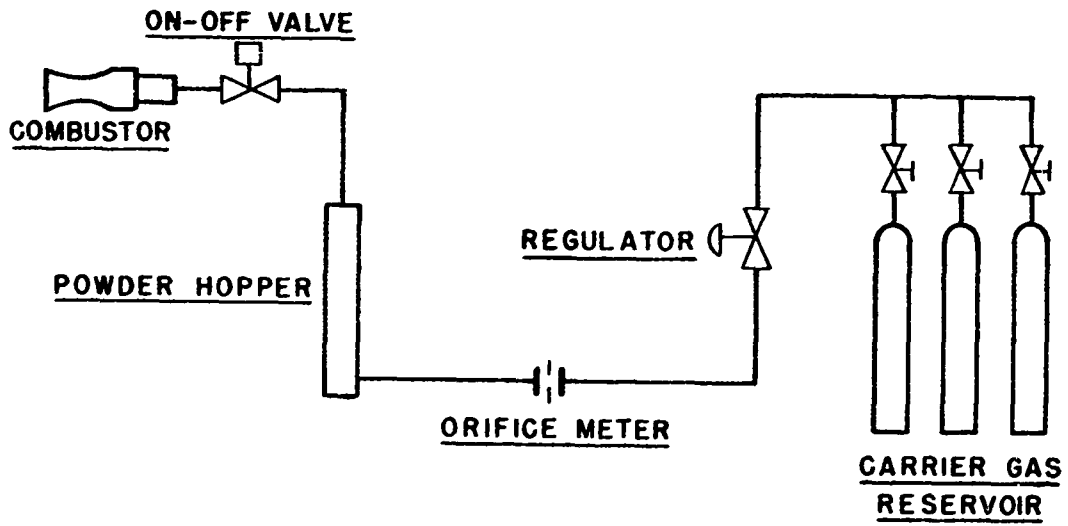


Figure 4. Powder injection system schematic.

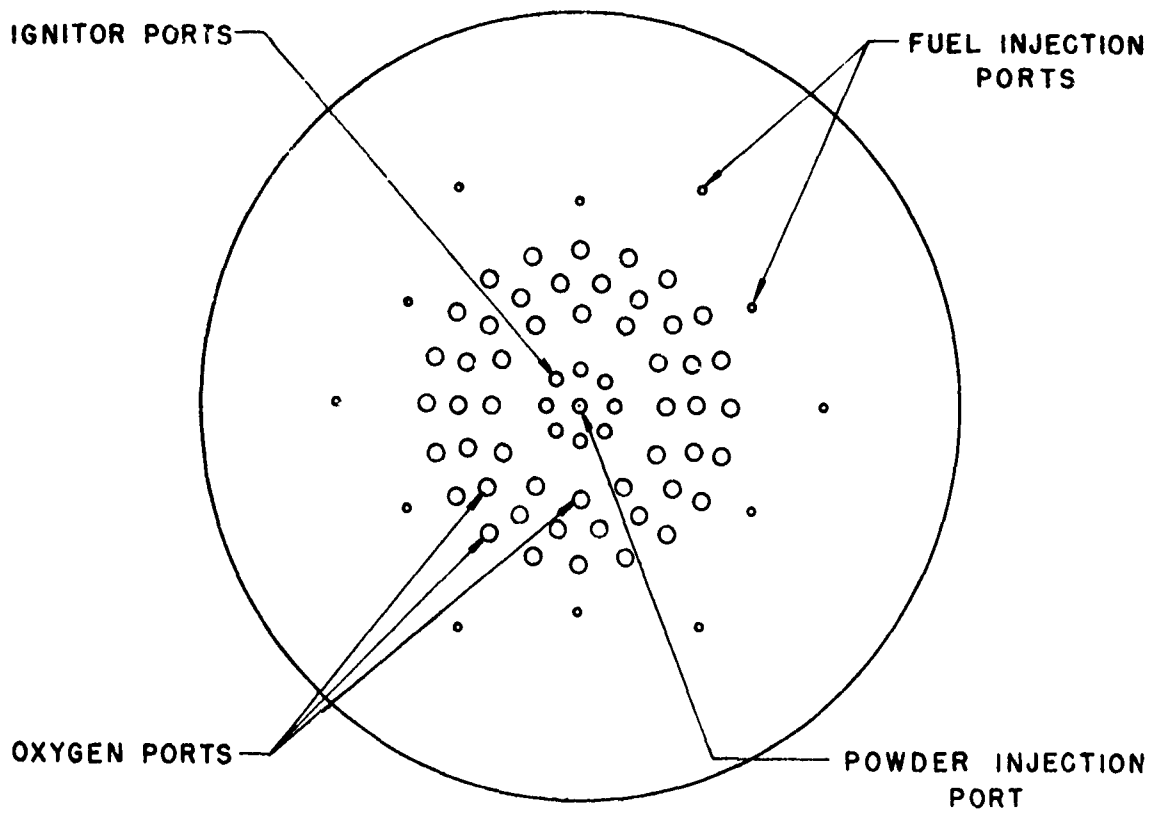


Figure 5. Propellant injection pattern with axial powder injection port.

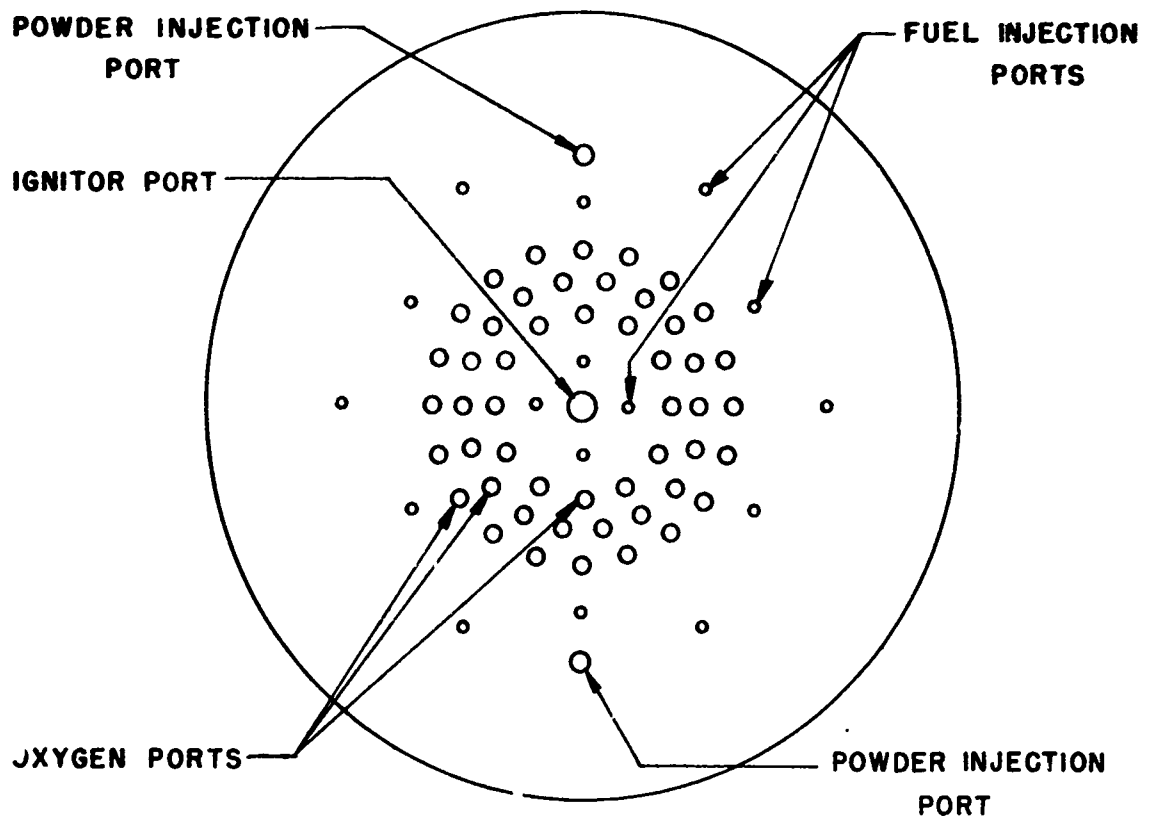


Figure 6. Propellant injection pattern with powder injection ports on outer perimeter.

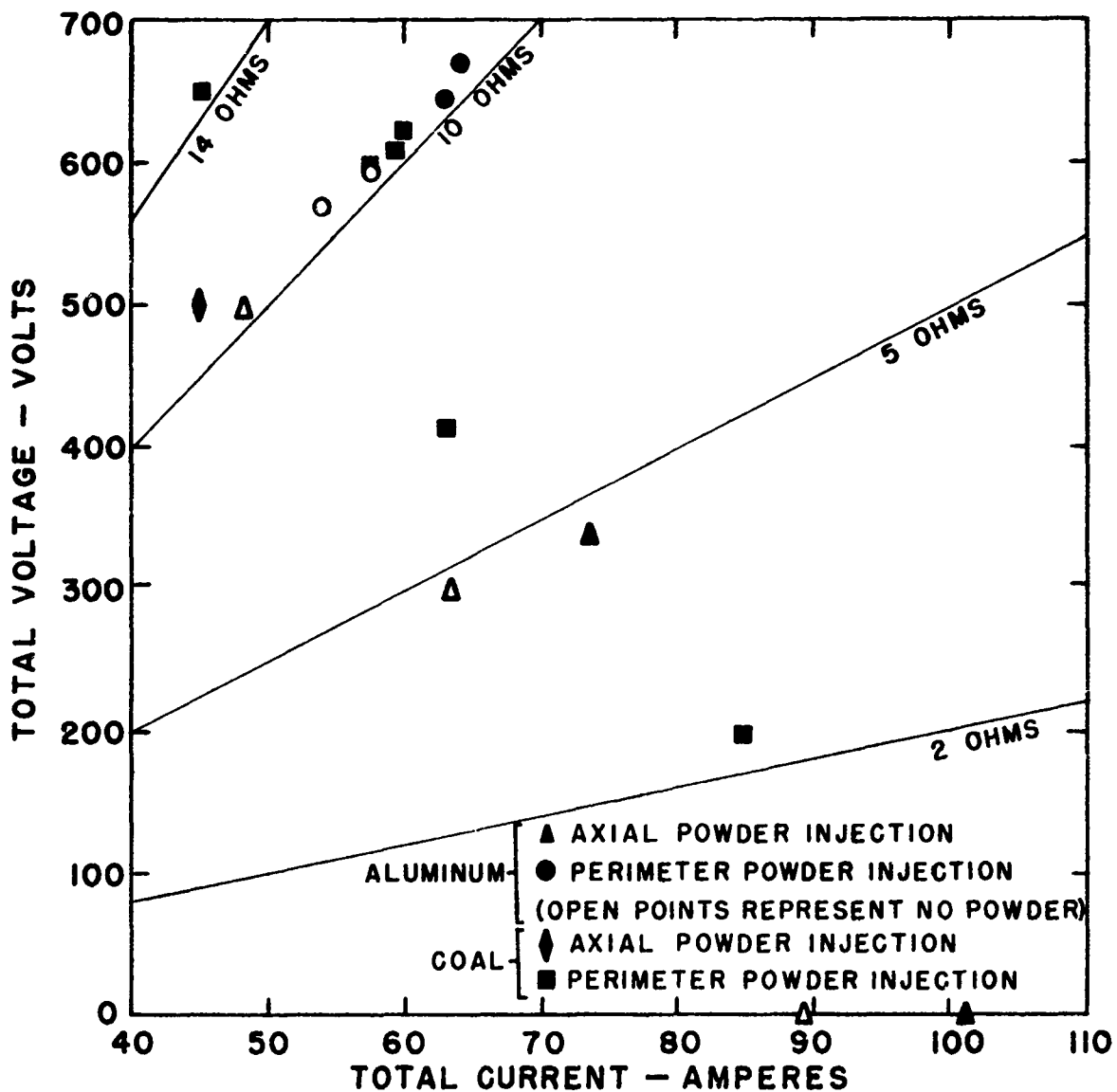


Figure 7. Voltage-current characteristics of a 60° wall generator using various powdered fuel additives.

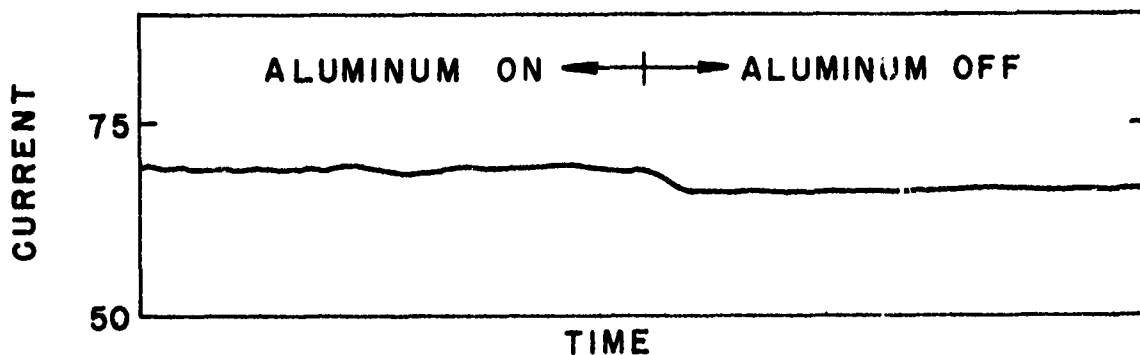


Figure 8. Oscillograph trace of total load current from 60° wall generator with aluminum injection interruption.

Figure 10. Axial variation of voltage drop for Hall generator.

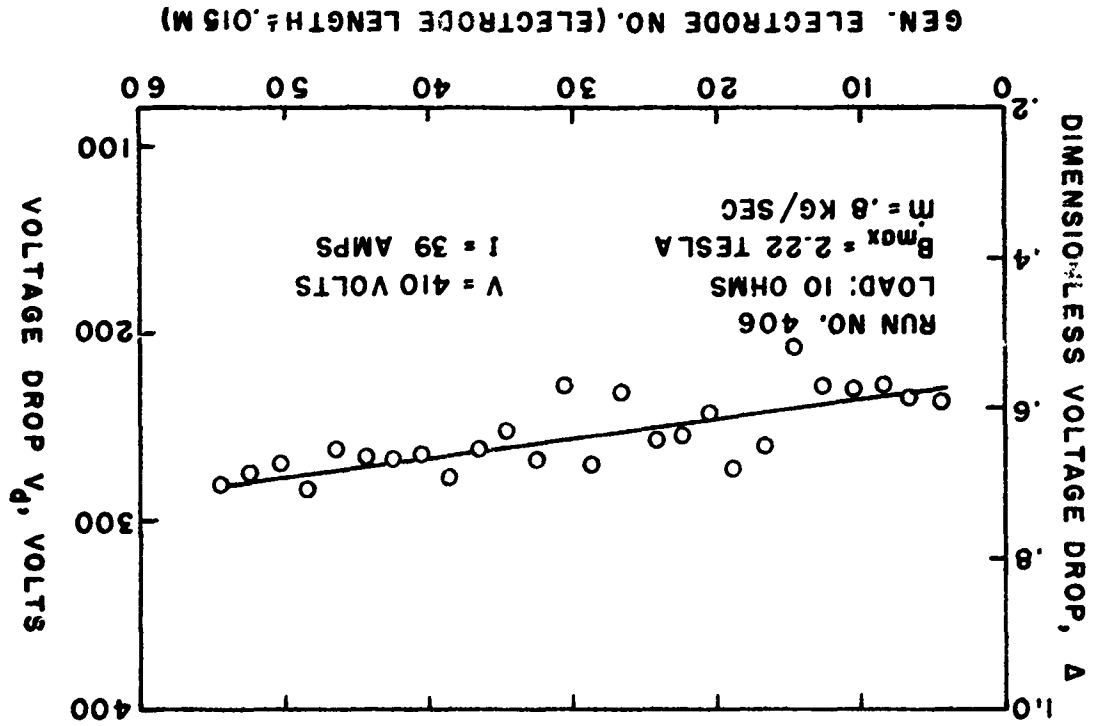
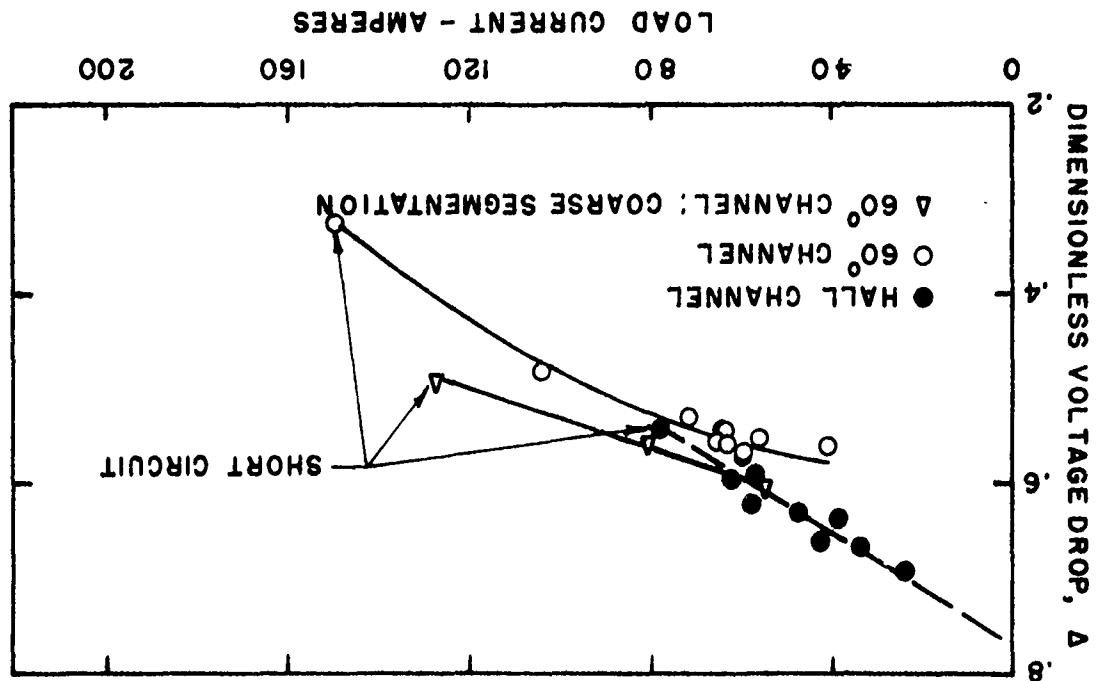


Figure 9. Dimensionless voltage drop as a function of load current.



## DOCUMENT-CONTROL DATA - R &amp; D

(Security classification of title, body of abstract and indexing annotation must be entered when the overall report is classified)

1. ORIGINATING ACTIVITY (Corporate author) UNIVERSITY OF TENNESSEE SPACE INSTITUTE TULLAHOMA, TENNESSEE 37388		2a. REPORT SECURITY CLASSIFICATION Unclassified	
		2b. GROUP	
3. REPORT TITLE FACTORS EFFECTING THE PERFORMANCE OF DIAGONAL CONDUCTING WALL OPEN CYCLE MHD GENERATORS			
4. DESCRIPTIVE NOTES (Type of report and inclusive dates) Scientific Interim			
5. AUTHOR(S) (First name, middle initial, last name) Y C L Wu L Crawford R Shanklin J Muehlhauser D Molnar J B Dicks			
6. REPORT DATE 4 February 1971	7a. TOTAL NO. OF PAGES 17	7b. NO. OF REFS 6	
8a. CONTRACT OR GRANT NO. F44620-69-C-0031	8b. ORIGINATOR'S REPORT NUMBER(S)		
b. PROJECT NO. 9561-00			
c. 61102F	9b. OTHER REPORT NO(S) (Any other numbers that may be assigned this report) AEOSR-TR-71-0853		
d. 681307			
10. DISTRIBUTION STATEMENT 1. This document has been approved for public release and sale; its distribution is unlimited.			
11. SUPPLEMENTARY NOTES PROCEEDINGS Fifth Int. Conf on Magnetohydrodynamic Elec Power Generation 19-23 Apr 71 Munich Germany		12. SPONSORING MILITARY ACTIVITY AF Office of Scientific Research (NAE) 1400 Wilson Boulevard Arlington, Virginia 22209	
13. ABSTRACT A systematic study has been undertaken to attempt to evaluate gross factors effecting the overall performance of series connected generators. These factors include combustor performance, chemistry, magnetic field strength, Mach number, and electrode segmentation. The scaling law for the magnetic field is of the form $(B-V_d/ud)^2$ . Dimensional scaling was investigated by varying the segmentation that when the electrode length to channel height. The results show that when the electrode length divided by the channel height is changed from the neighborhood of .12 to the neighborhood of .25 then the generator power output decreases by 15 percent over the entire load spectrum. Other studies involving gross generator behavior include an investigation of the effect resulting from the deposit of aluminum oxide and other combustion materials on the walls of the generator. No deterioration of performance was noted during this process. The addition of the powdered aluminum improved the generator performance. During the course of the experimental study, it was found that both the injector head and combustor are very critical to the performance of the generators.()			

14 KEY WORDS	LINK A		LINK B		LINK C	
	ROLE	WT	ROLE	WT	ROLE	WT
DIAGONAL CONDUCTING WALL OPEN CYCLE MHD GENERATORS						
PLASMA DYNAMICS						
ELECTRIC POWER GENERATION						
MHD POWER GENERATOR PERFORMANCE						
CHEMICALLY-DRIVEN MHD ELECTRIC POWER GENERATORS						
SERIES CONNECTED MHD GENERATORS						
MHD CHANNEL SCALING LAWS						